Research Article

iMedPub Journals
www.imedpub.com

Journal of Nanoscience & Nanotechnology Research

2018
Vol.2 No.1:1

Microstructural Behavior of Ti6Al4V during Room Temperature Deformation

Gajanan Kulkarni[1*], Vijay Hiwarkar[2], Jitendra Patil[1] and Rajkumar Singh[1]

[1]Bharat Forge ltd, Pune, Maharashtra, India

[2]Department of Materials Engineering, Defence Institute of Advance Technology, Pune, Maharashtra, India

[*]**Corresponding author:** Gajanan Kulkarni, Bharat Forge Ltd., Pune 411036, Maharashtra, India, Tel: 020-67042777; E-mail: Gajanan.kulkarni@bharatforge.com

Received: March 25, 2017; **Accepted:** April 03, 2018; **Published:** April 07, 2018

Citation: Kulkarni G, Hiwarkar V, Patil J, Singh R (2018) Microstructural Behavior of Ti6Al4V during Room Temperature Deformation. J Nanosci Nanotechnol Res Vol.2: No.1: 1.

Abstract

This study investigates the effect of room temperature deformation on the microstructural behavior of Ti6Al4V alloy. To study this, room temperature uniaxial compression test was carried out at low strain rate of 0.01 s-1 with increase in 5% stepwise degree of deformation up to fracture. At each stage of the deformation, Stress strain curve was correlated with change in microstructure .Microstructural evolution and grain Fragmentation are mapped at each stage of deformation with the help of EBSD and OPTICAL microscopy. Fracture of material occurs within 30% of deformation and exhibit grain refinement. Flow stress increases with increase in deformation and indexed in terms of Increase in strain hardening exponent and hardness. EBSD mapping and Microstructural analysis confirms Alpha phase fragmentation and grain size reduction.

Keywords: Ti-6Al-4V, deformation, Electron backscattered diffraction (EBSD), Hardness

Introduction

Titanium is the transition metal having hexagonal close pack structure (HCP) at room temperature [1]. Ti-6Al-4V is the most commonly used α+β titanium alloy. The properties of titanium are high strength to weight ratio and excellent corrosion resistance which makes this alloy most commonly used in the fields of defence, marine and aerospace applications [2]. Mechanical properties of Ti6Al4V alloy is mainly dependent on the processing parameters like strain rate and temperature [3]. Due to low volume fraction of the beta (BCC) phase, deformation behavior of the two phase alloy is mainly influenced by alpha phase [4]. During processing the evolution of the texture and microstructure mainly takes place due to the majority of the plastic strain which is accommodated by alpha phase [5]. In HCP crystal structure, Slip and Twin activity promotes the plastic deformation [6]. In commercially pure titanium, the plastic deformation mainly takes place by twinning [7]. High solute content and presence of the Ti3Al precipitates causes suppression of the twinning in Ti6Al4V alloy [9].

Strain rate also affect the twinning. At low temperature and high strain rate, deformation mainly takes place by twinning [10, 11]. Alloying element mainly influence the deformation behavior of the Ti6Al4V alloy. In Ti6Al4V, as the Hydrogen content increases the tensile property decreases and compressive property increases [12]. Grain size also affects the occurrence of deformation twinning [13]. Twinning is mostly seen in larger grains than small grains.

Tirry et al observed that, after shear deformation of the ti6al4v sheet material, presence of the twinning is less [14]. P. Krakhmalev et al. also studied and observed that, after deformation of the Ti6Al4Vproduced by SLM microstructure changes to fully martensite and high dislocation density was found [15]. D.G.L. Prakash et al. also found in the detailed study of the deformation of the Ti6Al4V at slow strain rate that, with increasing plastic deformation the rate of twinning increases [16].

From above summary it was found that, the microstructure evolution during deformation is correlated with slip and twin activity. The main purpose of this work is to find out the relationship between flow stress and microstructural evolution at each stage of deformation.

Experimental Details

In this study, the compression specimens of size Ø8 mm×12 mm were machined from Annealed Ti-6Al-4V bar having equiaxed microstructure. Machining direction of sample was parallel to rolling direction. Chemical composition of as received material is listed in **Table 1**.

The uniaxial compression test was carried out on servo hydraulics MTS machine 0.01 s-1 strain-rates at room temperature. The samples were deformed with 5% stepwise degree of deformation up to fracture.

For microstructural characterization, deformed samples were mirror polished and etched with Krolls reagent. For EBSD study, samples were electro-polished by electrolyte containing 90% of methanol and 10% perchloric acid. The electro-polishing was done at voltage of 26V for 10sec. The scanned area for EBSD was 300 µm^2 and step size of 0.3µm. XRD was done on the pan-analytical MRD machine.

Table 1 Chemical composition of the as received sample in wt %.

Chemical elements	Al	V	Fe	O	C	N	Ti
Wt%	6.4	4	0.16	0.18	0.02	0.01	Balance

Stress strain behavior

True stress strain curves and engineering stress strain curves were recorded during the room temperature deformation of the Ti6Al4V alloy. True stress strain curves, engineering stress strain curves and strain hardening exponent (n) are shown in **Figure 1**.

The samples were deformed with 0.01 s-1 strain rate up to 30% deformation. It was observed that, as the deformation increases the flow stress increases. According to dislocation theory, as the plastic deformation increases the dislocations density increases, which results in flow stress increases with increase in deformation. At slower strain rate and at early stage of deformation, as the dislocation density is less they can easily glide slip planes and does not get hindered by obstacles [17].

After progressive deformation, due to rapid multiplication of the dislocations flow stress increases. Strain hardening exponent (n) is used to indicate the effect of deformation on the work hardening behavior of Material. It is derived from the slope of the true stress strain curve. Higher the strain hardening exponent, higher is the work hardening effect [18].

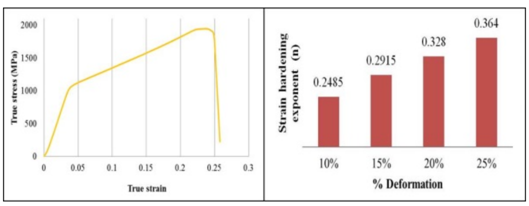

Figure 1 Stress strain curves a) Engineering stress strain curves b) True stress strain curves c) strain hardening exponent (n) of Ti6Al4V alloy.

Strain hardening exponent (n) of the deformed and as received sample is shown **Figure 1b**. It was observed that, Strain hardening exponent (n) increases with increase in deformation. At 25% deformation, higher work hardening was observed. After 25% deformation sample starts cracking and flow stress decreases.

Results and Discussion

Microstructural evolution

Optical micrograph, EBSD IPF map and grain size of as received samples of TI6Al4V alloy are shown in **Figure 2**. **Figure 2a** shows microstructure of as received sample of the annealed Ti6Al4V bar with equiaxed alpha and finely distributed beta grains are observed. Beta phase was restricted at triple points. EBSD mapping shows that, as received sample of Ti6Al4V with average grain size is 10µ contains 86% of alpha phase and 14% beta phase. As the volume fraction of beta phase is negligible, majority of plastic strain is accommodated by alpha phase. Deformation behavior of the as received alloy was characterized by EBSD map and Microstructural characterization.

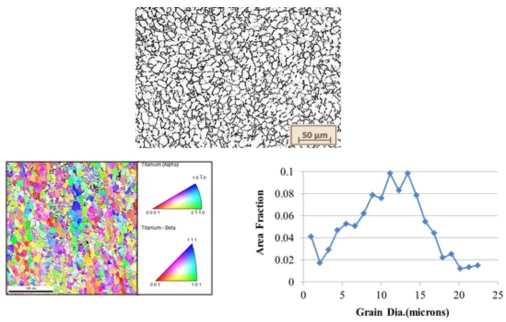

Figure 2 a) optical micrograph b) EBSD IPF map c) Grain size of as received sample of Ti6Al4V alloy.

Effect of plastic deformation on the grain size and average grain size of the Ti6Al4V as received and deformed samples is shown in **Figure 3**. Grain size data was obtained from EBSD. It was observed that, average grain size and grain size reduces with increasing deformation. Volume fraction of small size grains increases with increase in deformation. At 25% deformation, high volume fractions of smaller grains are observed. It indicates that, grain refinement increases with increasing strain. As the twins were not observed in microstructure, these results are only speculated in terms of dislocation activity in low stacking fault energy material. The process involves emission of partial dislocations from α/β interface. With increasing strain, these partial dislocations forms planar network by cross slip. The planar dislocation arrays separate the individual grains in to sub grains [19] .It was observed that, volume fraction of the Low Angle Grain Boundaries (LAGB's) increases with increase in deformation. Effect of increasing strain on volume fraction of the low angle grain boundaries is shown in **Figure 3c.** Higher volume fraction of the LAGB's are formed at 25% deformation. This indicates that, high volume fraction of the small equiaxed grains are formed at 25% deformation. The emitted partial dislocations from triple point of beta phase separates the individual alpha grains in to small equiaxed grains.

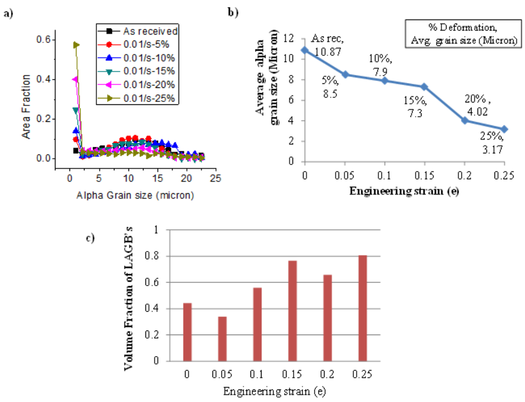

Figure 3 a) Alpha grain size b) Avg. alpha grain size c) Volume Fraction of LAGB's (Low Angle Grain Boundaries) of the as received and deformed samples of the Ti6Al4V with 0.01/s strain rate.

Hardness of the Ti6Al4V as received and deformed samples is shown in **Figure 4**. It was observed that, Hardness of the samples increases with increasing deformation. At 25% deformation, highest hardness of 375Hv was observed. This Increase in hardness results from hall petch mechanism and fank read source mechanism. As the deformation increases, Grain boundary area increases (Refer **Figure 4b**).The dislocations generated during plastic deformation are hindered at grain boundary area [20]. Hindering causes the dislocations become immobile and piled up at grain boundary area. Increase in dislocation density results in high hardness.

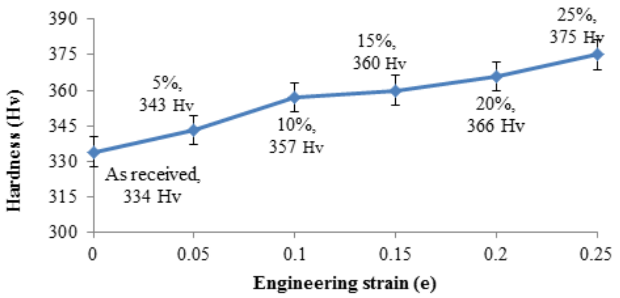

Figure 4 Hardness of the as received and deformed samples of the Ti6Al4V with 0.01/s strain rate.

Figure 5 shows the microstructure evolution at each stage of deformation. It was observed that, as the deformation increases the alpha grain fragmentation increases. At 15% deformation, higher Alpha grain fragmentation was observed (ref. **Figure 4b**). At 25% deformation, higher volume fractions of smaller grains with fragmented grains are formed.

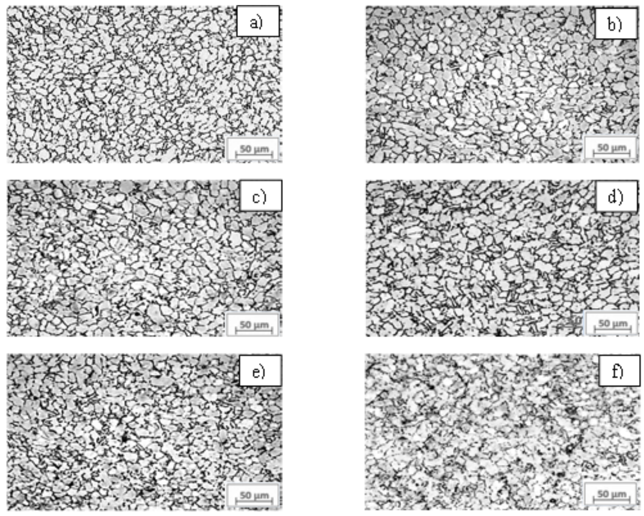

Figure 5 Microstructures of the as received and deformed samples , a) As received sample b) 5% deformed c) 10% deformed d) 15% deformed e) 20% deformed f) 25% deformed.

Conclusion

Room temperature plastic deformation of Ti6Al4V with very slow strain rate of 0.01s-1 was studied and investigated. Electron backscatter diffraction (EBSD) and Optical microscopy were used for the analysis of material deformation behavior. The main findings are as:

- Compression test result shows that, flow stress and Strain hardening exponent (n) increases with increasing deformation. Work hardening phenomenon was observed.
- Microstructural characterization and grain size data confirms that, alpha grain fragmentation and grain distortion increases with increasing strain. Grain refinement was observed at higher strain.
- Hardness data was correlated with microstructural evolution. It indicates that, hardness of the sample increases by Hall petch mechanism. Peak hardness was observed at 25% deformation.

References

1. Boyer R, Welsch G, Collings EW (1994) Materials Properties Handbook: Titanium Alloys, Metals Park, OH, ASM.
2. Leynes C, Peters M (2003) Titanium and Titanium alloys: Fundamentals and Applications. Wiley- VCH, UK.
3. Chiou ST (2007) Effects of strain rate and temperature on the deformation and fracture behaviour of titanium alloy. Mater Trans Japan 48: 2525-2533
4. Dunst D, Mecking H (1996) Zeitschrift Fuer Metallkunde. 87: 498-507.
5. Lee WS (2008) The strain rate and temperature dependence of microstructural evolution of Ti–15Mo–5Zr–3Al alloy. J Mater Sci 43: 1568-1575

6. Nemat-nasser S (1999) Mechanical properties and deformation mechanisms of a commercially pure titanium. Acta Mater 47: 3705.
7. Lee WS, Lin CF (1998) Plastic deformation and fracture behaviour of Ti–6Al–4V alloy loaded with high strain rate under various temperatures. Mater Sci Eng A 241: 48-59.
8. Prakash DGL, Ding R (2010) Deformation twinning in Ti-6Al-4 V during low strain rate deformation to moderate strains at room temperature. Mater Sci Eng A 527: 5734-5744.
9. Castany P, Pettinari-Sturmel F (2007) Experimental study of dislocation mobility in a Ti–6Al–4V alloy. Acta Materialia 55: 6284-6291.
10. Chichili DR, Ramesh KT (1998) The high-strain-rate response of alpha-titanium: experiments, deformation mechanisms and modelling. Acta Mater 46: 1025-1043.
11. Follansbee PS, Gray GT (1989) An analysis of the low temperature, low and high strain-rate deformation of Ti−6Al−4V. Metall Mater Trans 20: 863-874.
12. Sun Z (2010) Investigations on cold deformation mechanisms of the hydrogenated Ti–6Al–4V alloys. Mater Sci Eng A 527: 1003-1007.
13. Saxena AK (2015) Effect of grain size on deformation twinning behavior of Ti6Al4V Alloy. Mater Sci For 830: 337-340.
14. Tirry W, Coghe F (2010) A multi-scale characterization of deformation twins in Ti6Al4V sheet material deformed by simple shear. Mater Sci Eng A 527: 4136-4145.
15. Krakhmalev P (2016) Deformation behavior and microstructure of Ti6Al4V manufactured by SLM. Phy Pro 83:778-788.
16. Ramesh KT (2002) Effects of high rates of loading on the deformation behavior and failure mechanisms of hexagonal close-packed metals and alloys. Metall Mater Trans A 33: 928.
17. Samajdar I (2007) Thermo-mechanical processing of metallic materials. Elsevier, USA.
18. Afrin N (2007) Strain hardening behavior of a friction stir welded magnesium alloy. Scripta Materialia 57: 1004-1007.
19. Azadmanjiri J (2014) Critical reviews in solid state and materials sciences. 18: 1-18.
20. Jung BB (2013) Effect of grain size on the indentation hardness for polycrystalline materials by the modified strain gradient theory. Int J Sol Str 50: 2719-2724.